J. Biomed. Eng. Res
Vol. 21, No. 4, 373-384, 2000

스폰지 뼈의 Remodeling 예측을 위한 체적 변형률을 이용한 유한요소 알고리즘

김 용[1,2] and 벤더비 레이[1,2]

정형외과/기계공학과 위스콘신 주립대, 미국

(2000년 2월 14일 접수, 2000년 7월 10일 채택)

A Finite Element Simulation of Cancellous Bone Remodeling Based on Volumetric Strain

Young Kim[1,2], Ray Vanderby[1,2]

[1]Department of Orthopedic Surgery, [2]Department of Mechanical Engineering
University of Wisconsin-Madison, G5/332 Clinical Science Center
600 Highland Avenue, Madison, WI 53792-3228

(Received February 14, 2000, Accepted July 10, 2000)

요 약 본 연구의 목적은 체적 변형률 (volumetric strain) 에 의한 스폰지 뼈의 밀도를 예측하는 것이다. 스폰지 뼈의 내부에서 유체의 흐름을 고려하기 위하여 각각의 normal strain의 합을 체적 변형률로 정의 하였다. 체적 변형률의 경계조건에 대한 민감한 반응은 스폰지 뼈의 밀도를 예측하도록 하였다. 이러한 이론적 배경을 유한요소법 (finite element method)에 적용시켜 대퇴골 (femur) 과 척추 (spine) 의 스폰지 뼈에서의 밀도를 예측하였다. 예측된 뼈의 밀도는 실험적 데이터와 매우 유사하였다 (Wolff 1892, Keller *et al* 1989, Cody *et al* 1992) 뼈의 밀도의 함수인 뼈의 탄성계수와 강도 또한 실험적 결과와 매우 유사하였다 (Keller *et al* 1989, Carter and Hayes 1977) 본 연구에서 정립된 알고리즘은 스폰지 뼈의 밀도를 예측하는데 있어서 수렴성과 민감성이 우수하였다 따라서 본 연구의 컴퓨터 알고리즘은 스폰지 뼈의 밀도예측에 있어서 매우 유용한 방법이 될 것이다

Abstract : The goal of this paper is to develop a computational method to predict cancellous bone density distributions based upon continuum levels of volumetric strain. Volumetric strain is defined as the summation of normal strains, excluding shear strains, within an elastic range of loadings. Volumetric strain at a particular location in a cancellous structure changes with changes of the boundary conditions (prescribed displacements, tractions, and pressure) This change in the volumetric strain is postulated to predict the adaptive change in the bone apparent density. This bone remodeling theory based on volumetric strain is then used with the finite element method to compute the apparent density distribution for cancellous bone in both lumbar spine and proximal femur using an iterative algorithm considering the dead zone of strain stimuli. The apparent density distribution of cancellous bone predicted by this method has the same pattern as experimental data reported in the literature (Wolff 1892, Keller *et al*. 1989, Cody *et al* 1992) The resulting bone apparent density distributions predict Young's modulus and strength distributions throughout cancellous bone in agreement with the literature (Keller et al 1989, Carter and Hayes 1977). The method was convergent and sensitive to changes in boundary conditions Therefore, the computational algorithm of the present study appears to be a useful approach to predict the apparent density distributions of cancellous bone (i.e a numerical approximation for Wolff's Law)

Key words : Apparent density, Bone remodeling, Volumetric strain, Strain energy

INTRODUCTION

Ever since Wolff published his observations on trajectory patterns in cancellous bone in 1892 (Wolff 1892), bone remodeling has been a topic of great biomechanical

통신저자 Young Kim, 15-51 Hwayang-dong, Kwangjin-gu Seoul, 143-130, South Korea
Tel. (016)244-2156, Fax. (02)580-5350
E-mail. ykim8@hotmail.com

interest. Wolff suggested that formation and resorption of trabecular bone depend on the local stress state resulting from the load environment. Several investigators have suggested that there is a normal strain range correlated with bone remodeling equilibrium in which there is no net apposition or resorption of the bone (Frost 1987, Cowin 1984). The cancellous bone structure, as defined by its local apparent density, achieves an equilibrium state when the stimulus stays in this normal range. When the stimulus stays below or exceeds this normal range, cancellous bone changes its apparent density, adapting to the mechanical environment. Churches and Howlett(1981) reported that axial loading conditions are more beneficial than bending as a stimulus for bone remodeling, which might mean that shear strains under bending loads are less important for bone remodeling. Wolff(1892) observed femoral cancellous bone that had been subjected to bending loads, showing examples of cancellous bone trajectories consistent with directions of principal stress(Fig. 1). Several investigators reported that an appropriate compressive load is beneficial to fracture healing, whereas excessive compression or any axial torsion is harmful to healing(Grundenes and Reikeras 1993). Based on these experimental observations, it appears that within normal physiologic levels of loadings, axial strains or normal strains are the more dominant biomechanical factors for bone remodeling, whereby shear strains are less relevant to bone remodeling. Current bone remodeling theories use strain energy density (Goel *et al.* 1995) or effective stress (Carter *et al.* 1989) as a stimulus for bone remodeling. These theories include shear strains, although bone remodeling based on an isolated shear strain has never been observed.

Many investigators (Antonsson and Mann 1985, Capozzo *et al.* 1975, Churches and Howlett 1981, Lanyon and Rubin 1985) suggest that cancellous bone distributes itself and remodels as a function of strain magnitude for similar load frequencies, showing that this interpretation of Wolff's Law is supported by many experimental studies. Consider, for example, lumbar vertebral bodies and the proximal femur. Spinal loads resulting from body weight or muscle contraction are constantly applied to the lumbar spine, keeping the nucleus pulposis under a considerable level of pressure. These spinal loads cause compressive strains in the axial direction of the vertebral body to be dominant. These strains, in turn, are likely to be the dominant biomechanical factors that regulate density distribution and remodeling of cancellous bone. Thus, it is reasonable to assume that axial compressive strain can be used to predict the apparent density distribution of cancellous bone in the vertebral bodies of the human spine. However, in a proximal femur, axial compressive loads are coupled with bending, producing a more complex strain distribution. Both loads probably affect cancellous bone density distribution and remodeling. Ergo, all normal strains, which are the components of a volumetric strain, should be included when considering a mechanical stimulus for cancellous bone distribution and remodeling in the proximal femur.

Several analytical methods have been used to predict the distribution of the cancellous bone apparent density or bone remodeling. Using finite element method, Goel *et al.* (1995) showed that Young's modulus varies with anatomic region on cancellous bone of human lumbar spine based on a strain energy density theory, requiring many unknown parameters, and a uniform homeostatic strain energy density distribution. Carter *et al.* (1989) predicted the bone apparent density distribution in an adult proximal femur based on effective stress in order that the principal material directions do not necessary correspond to the principal stress direction. Carter and associates used a formula that calculated a stimulus based upon magnitude and number of load cycles/day. Carter(1987) established an algorithm of bone remodeling to represent morphogenesis, growth, regeneration, maintenance and degeneration, assuming that shear stresses induce bone gain and that hydrostatic stresses inhibit bone gain. Weinans *et al.* (1994) explored effects of fit and bonding characteristics of femoral stems on bone remodeling based on the strain energy density. Cowin and Hegedus (1976) suggested that the apparent density of cancellous bone structure is determined from strain but, they didn't need to show that how the apparent density is updated. A recent study(Turner *et al.* 1997) used a uniform strain criterion using the principal strains for prediction of apparent density in the proximal femur, showing that the algorithm converged upon an apparent density distribution that was similar to anatomically observed distributions. Fischer *et al.*(1997) showed that a node based remodeling algorithm can converge to a unique density distribution.

The goal of the present study was to explore a different approach to predict bone remodeling. A remodeling theory is formulated for cancellous bone based on a volumetric strain criterion. This theory is implemented and solved using the finite element method. This theory is demonstrated by applying it to a human proximal femur and to three vertebrae in the human lumbar spine. Apparent density distributions predicted by the model are com-

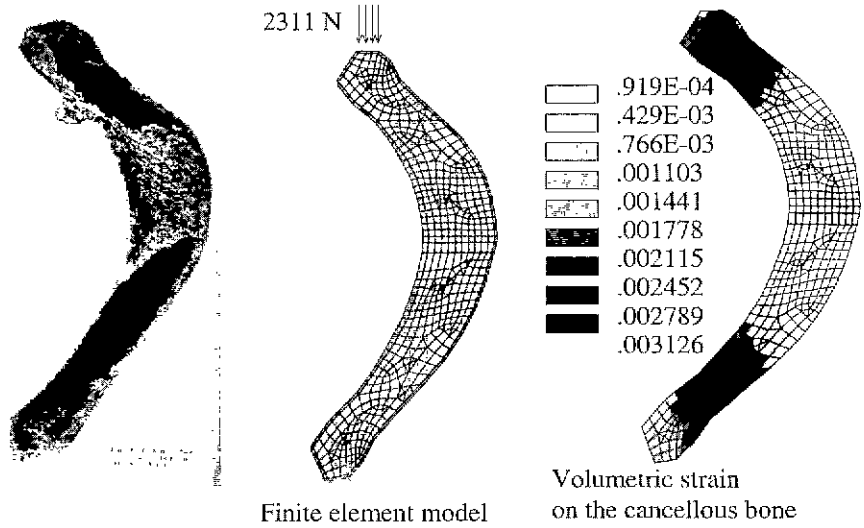

Fig. 1. Finite element model of a curved femoral diaphysis The right plot is a curved femur referred from Wolff(1892) The femur was modeled as shown on the central plot. The left plot represents a volumetric strain distribution based on the bone remodeling theory. The distribution of volumetric strain in the middle region of the model shows similar trends to the density distribution of the curved femur on the right plot

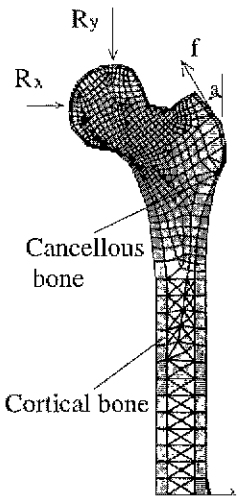

Fig. 2. Finite element model of a normal proximal femur with boundary conditions(a=31 degrees, reaction forces f=1696.3 N, R_x=873.7 N, and R_y=2311 N)

pared to those reported in the literature.

METHODS

The finite element method was used to predict apparent density distributions of cancellous bone in the human lumbar spine and femur. Two two-dimensional femur models and a three-dimensional spine model were generated (Fig 1, 2, 4, Table 1) The models were analyzed with a general purpose finite element package, ANSYS (Version. 5.1a, Swanson Analysis Systems, Inc., Houston, PA).

1. Femur models

Two femur models were considered in the present study, a curved femoral diaphysis(Fig. 1) adapted from Wolff(1892) and a normal proximal femur(Fig 2) The geometry of the normal femur model was based on Wolff (1892) and Carter *et al.*(1989) These models included both cortical and cancellous bone. These models used two -dimensional elements(PLANE42) defined by four nodes having two degrees of freedom(i.e. translations in the nodal x and y directions) at each node. In the curved femur model and the normal femur model, an initial uniform Young's modulus(100 MPa) was assumed throughout the cancellous bone with a Poisson's ratio of 0.2 The loading boundary conditions were based upon a body weight of 100 kg according to the literature(Cowin 1991). Reaction forces were applied to the normal femur model as shown on Fig. 2. A compressive load of 2311 N was vertically applied to the curved femur model in order to investigate cancellous bone density distributions(Cowin 1991)

2 Spine model(L3-L5)

The geometric data for the FEM modeling of L3-L5 motion segment were based on the recent literature(Panjabi *et al.* 1992, Grobler *et al.* 1993,Marchand and Ahmed 1990). The vertebral geometry was referred from Panjabi

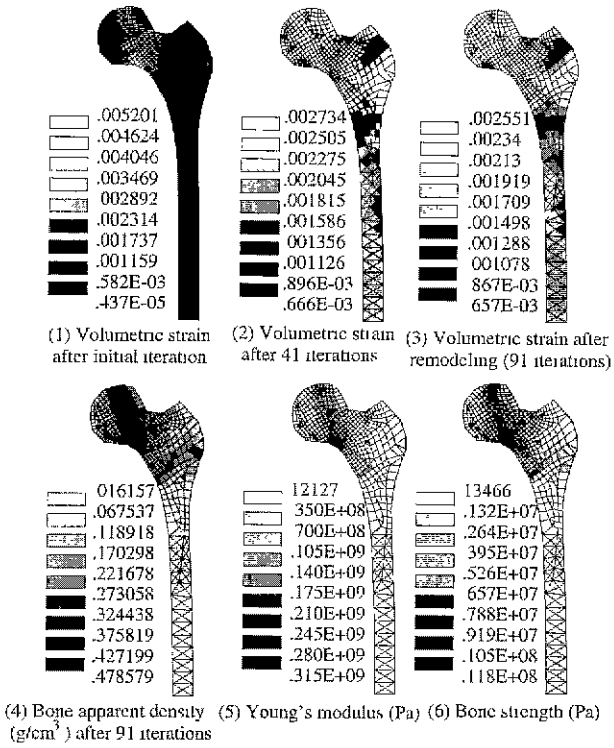

Fig. 3a. Remodeling processes based on the bone remodeling theory in the femoral cancellous bone. The initial range of volumetric strain was reduced and converged into the homeostatic range defined by Frost(1987) with increasing the iterations. At every iteration, the apparent density distribution was predicted. Based on the apparent density distribution Young's modulus and bone strength were predicted.

et al(1992). Geometry for the facet joint was referred from Panjabi *et al.*(1993) and Grobler *et al.*(1993). A lordotic angle for the normal spine model was assumed to be 3 degrees based on post-mortem data(Cox and Stevens 1985).

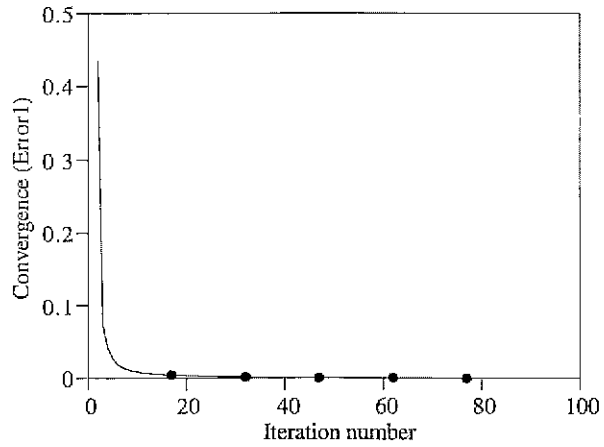

Fig. 3b. The convergence process with iterations for the proximal femur model.

In formulation of the three-dimensional finite element model of a lumbar spine(L3-L5), cortical bone, cancellous bone and posterior bone were modeled as three-dimensional isoparametric eight-node elements(SOLID45) defined by eight nodes having three degrees of freedom(i.e. 3 translations) at each node. The intervertebral disc was modeled as a composite materials with a series of fiber bands and a ground substance around the nucleus, similar to the recent literature(Goel *et al.* 1995, Shirazi-Adl *et al.* 1986). Irregularity of the annulus fibrosis was included according to the literature(Marchand and Ahmed 1990, Skaggs *et al.* 1994). The collagenous fibers in the annulus fibrosis and ligaments are bilinear materials which are very stiff in tension and very compliant in compression. These fibers were then modeled as cable elements(LINK 10) supporting tension only. The nucleus of the intervertebral disc was modeled as fluid elements(FLUID80) which are well suited to simulate the hydrostatic behavior and fluid/solid interactions associated with a normal nucleus pulposis. Facet articulations were modeled with gap elements(CONTAC52) which can support a compressive normal load to the surface. In this model an initial gap distance of 0.45 mm was assumed. Frictional force between opposing facets were assumed to be zero.

Material and mechanical properties of the normal spine model(Table 1) were obtained from the literature(Fyhrie and Schaffler 1994, Rice *et al.* 1988) where Young's modulus and strength of the cancellous bone are functions of bone apparent density(Carter *et al.* 1989). The bone apparent density varies with anatomic region in cancellous bone(Keller *et al.* 1989). In boundary conditions of the spine model, the inferior surface of the L5 vertebra was fixed. Muscle activation was ignored in this study. Compressive loads of 400 to 800 N were distributed on the superior surface of 1.58 cm^2 area.

3. Bone remodeling theory based on the volumetric strain

It is known that compression and tension produce a greater remodeling response in bone than any other load (Antonsson and Mann 1985, Capozzo *et al.* 1975, Churches and Howlett 1981). However, the difference in bone remodeling response between compressive strain and tensile strain is not well defined. There is little evidence of bone remodeling in response to changes in shear strain while

Table 1. Material properties of human lumbar spine (L3-L5) and human femur

Materials	Young's modulus(MPa)	Poisson's ratio	Apparent density ρ (g/cm^3)
Spine model			
Cortical bone[11,30]	12000	0.3	1.8
Cancellous bone[11,30]	$2875\rho^3$	0.2	0.11-1.2
Posterior bone[30,31]	3500	0.25	1.8
Cartilaginous endplate	24	0.4	
Annulus matrix[19,20]	4	0.47	
Annulus fiber[19,20]	59-136		
Nucleus	1667.7,bulk modulus	0.4999	
Ligaments[30]	7.5-59	0.6-22.4, Cross-sec. area (mm^2)	
Femur model			
Cortical bone[30,31]	17000	0.3	1.9
Cancellous bone	$2875\rho^3$	0.2	0.11-1.2

there are many reports showing bone remodeling under changes in normal strains(Antonsson and Mann 1985, Capozzo *et al.* 1975, Churches and Howlett 1981) It is therefore assumed that shear strains are not a dominant factor in bone remodeling and can be ignored. In this study, volumetric strain from a rectangular coordinate system is postulated to be the stimulus for bone remodeling. Implementing this computationally is based on three assumptions:

1) The time interval required for changes in mass of cancellous bone($\Delta t_{remodel}$) is much longer than the time interval for physiologic loadings(Δt_{load}).

2) A small but finite region of cancellous bone undergoes strains with physiologic loading that consequently produce temporary(Δt_{load}) changes in volume and apparent density in a Lagrangian sense. These volumetric changes

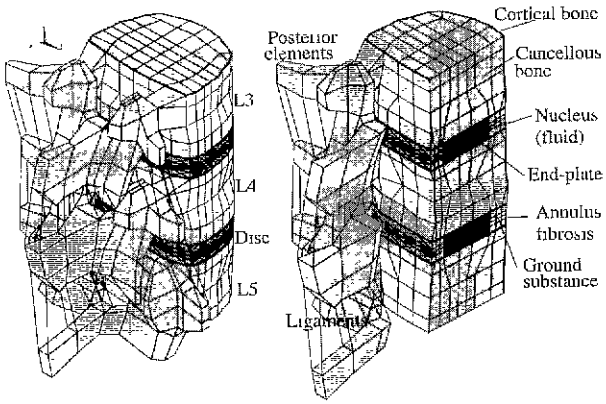

Fig. 4. Finite element model of the normal spine (L3-L5)

establish a homeostatic level of apparent bone density for a homeostatic range of normal volumetric strain. An increase or decrease from this critical value of volumetric strain will temporarily increase or decrease the level of apparent density(in a Δt_{load} interval). It is assumed that the remodeling response for a continued alteration in loadings, (in a $\Delta t_{remodel}$ interval) will change the unloaded local apparent density to be equivalent to that induced during the Δt_{load} interval

3) The absolute magnitude of normal strains is assumed to control the remodeling response. That is, tensile and compressive strains inducing volume change will be assumed to be the same factors in bone remodeling.

Based on first two assumptions, an iterative equation can be obtained.

$$\rho V = M = \text{constant} \quad (0 < t < \Delta t_{load}) \tag{1}$$

where ρ is density, V is a volume, and M is mass During a short loading interval(Δt_{load}), small changes in strain can alter the volume with corresponding small increases in the local apparent density If Equation 1 is differentiated to time,

$$V\frac{\partial \rho}{\partial t} + \frac{\partial V}{\partial t} = 0$$

$$\frac{d\rho}{\rho} = -\frac{dV}{V} \tag{2}$$

Equation 2 relates bone apparent density change and

the volume change over a loading interval. For small displacements, dV/V can be approximated by volumetric strain consisting of normal strains, that is,

$$\frac{d\rho}{\rho} \approx \varepsilon_{xx} + \varepsilon_{yy} + \varepsilon_{zz} \tag{3}$$

Equations 2 and 3 and the third assumption can be expressed

$$d\rho = -\rho(\varepsilon_{xx} + \varepsilon_{yy} + \varepsilon_{zz}) \tag{4}$$

$$d\rho = \rho\,\varepsilon_v, \text{ if } \varepsilon_v = -(C_x\varepsilon_{xx} + C_y\varepsilon_{yy} + C_z\varepsilon_{zz}) \tag{5}$$

where, strain coefficients c_x, c_y, c_z are 1.0 if the corresponding strain components are negative. Otherwise, the coefficients are assumed to be -0.1~-1.0. These assumption will be necessary to distinguish the tensile strain and the compressive strain because the difference between them would exist in bone remodeling. In this study the strain coefficients are assumed to be -1.0 according to the third assumption. The volumetric strain is modified into ε_v which is always positive, in order to develop a stimulus of remodeling. Equation 5 represents the short term change in bone density due to a loading as well as the incremental bone change that should occur by remodeling to compensate for this volumetric change.

It is assumed that over a period of time consistent with bone remodeling($\Delta t_{remodel}$), the current bone apparent density(ρ^{t+1}) can be described by the previous bone apparent density(ρ^t) and an incremental change($d\rho^t$) in bone apparent density.

$$\rho^{t+1} = \rho^t + d\rho^t \tag{6}$$

This change($d\rho^t$) in apparent density is assumed to be in response to a short term(Δt_{load}) load that changed the volumetric strain from a previous steady-state cancellous bone distribution. From Equations 5 and 6,

$$\rho^{t+1} = \rho^t(1+\varepsilon_v^t) \tag{7}$$

Equation 7 defines an incremental redistribution of the apparent density in cancellous bone. Prior to this increment there were previous increments of apparent density redistribution from the original value until volumetric strain had reached a reference value and apparent density had become homeostatic. Equation 7 then can be expanded so that bone apparent density can be calculated by the volumetric strain through a number of iterative time steps. Equation 7 can be rewritten as follows:

$$\rho^{t+1} = \rho^0(1+\varepsilon_v^0)(1+\varepsilon_v^1)(1+\varepsilon_v^2)\ldots\ldots(1+\varepsilon_v^t)$$

$$= \rho^0\prod_{n=1}^{t}(1+\varepsilon_v^n) \tag{8}$$

where ρ^0 is initial bone apparent density, and ε_v^0 is initial volumetric strain. With continuing iterations, Equation 8 converges to a new apparent density(ρ) for change of loading.

In order to consider the dead zone of strain stimuli in bone remodeling, a threshold level of volumetric strain(ε_{ref})isdefined. Frost(1987) suggested that bone normally receives between 200 and 2500 microstrain and the physiologic strain range is less than 4000 microstrain. Therefore, if ε_v is 2500-4000 microstrain, then bone apparent density will increase proportional to $\varepsilon_v - \varepsilon_{ref}$ for ε_{ref} = 2500 microstrain. If ε_v is less than 200 microstrain, then bone resorption will occur proportional to $\varepsilon_v - \varepsilon_{ref}$ for ε_{ref}=200 microstrain. But, if ε_v is in the range of 200-2500 microstrain, no remodeling will occur and $\varepsilon_{ref} = \varepsilon_v$. Equation 9 considers these conditions according to the magnitude of ε_v.

The frequency of loading has also been shown to affect remodeling(Antonsson and Mann 1985, Capozzo *et al.* 1975, Lanyon and Rubin 1985). Within a reasonable physiologic frequency range(less than 20 Hz), higher frequencies amplify the bone remodeling response while static loadings induce no remodeling(Antonsson and Mann 1985, Capozzo *et al.* 1975, Lanyon and Rubin 1985). The effect of frequency has then been implemented into the model. If a reference frequency of a dynamic cycle f_{ref}, and an arbitrary frequency of a dynamic cycle f, are assumed, Equation 8 is rewritten as follows,

$$\rho^{t+1} = \rho^0\prod_{n=1}^{t}(1+(\varepsilon_v^n\frac{f^n}{f_{ref}} - \varepsilon_{ref})C_m) \quad (0 < 20 \text{ Hz}) \tag{9}$$

where, ε_{ref} = 200 if ε_v < 200 microstrain

ε_{ref} = 2500 if ε_v > 2500 microstrain

$\varepsilon_{ref} = \varepsilon_v$ if 200 microstrain < $\varepsilon_v \le$ 2500 microstrain

Thus, higher frequency loads amplify the remodeling

response and lower frequency loads diminish it

In order to reduce the computational time, an amplification factor of C_m was introduced into Equation 9 Without C_m thousands of iterations were sometimes necessary to converge to density levels where $200 \leq \varepsilon_v \leq 2500$ microstrain(i.e. homeostatic range of the volumetric strain) throughout the structure The reason was that volumetric strain is on the order of 0.001 of the bone apparent density 1.0g /cm^3 The iterative solution of Equation 9 could now become divergent because of the amplification factor(C_m) To assure numerical stability, a convergence criterion was formulated and checked at every iteration (i). The convergence criterion, C_1, is defined as

$$\frac{\sqrt{\sum_{j=1}^{k}(\rho_j^{i+1}-\rho_j^{i})^2}}{\sqrt{\sum_{j=1}^{k}(\rho_j^{i})^2}} \leq C_1 \qquad (10)$$

The summation from 1 to k is over the total number of elements of cancellous bone. The accuracy of the converged solution depends on C_1 C_1 is expected to be less than 0.001 for convergence. Equation 10 is the ratio of a summation of the current incremental element densities to the summation of current element densities.

4 Initial density determination of the remodeling theory

Initial apparent density(ρ^0) is pre-assumed and the algorithm converges to an apparent density distribution consistent with the levels of ε_v. A good estimate of ρ^0 will greatly reduce the computation time. Therefore, the following method was developed to estimate ρ^0 for the spine model. Since axial compression is the most dominant load on the human lumbar spine, the axial compressive strain is the most dominant term in volumetric strain. For homeostasis of the vertebral cancellous bone, the axial strain should then approximate 200-2500 microstrain based upon Frost's observations (Frost 1987). If an apparent density distribution can be estimated to approximate a uniform axial value of 2500 microstrain throughout the cancellous bone, the pre-assumed apparent density should be close to the final converged value. This is accomplished by following a strain energy technique:

1) Initially, Young's modulus of the cancellous bone is assumed to be an arbitrary uniform value (E_1). An axial compressive loading is then applied to the normal spine model. After this initial iteration, an axial strain which is an initial strain in the vertical direction (y-axis shown in Fig. 1), ε_{y1}, is obtained, and the strain energy per volume over the cancellous bone is computed from

$$U_{initial} = \frac{1}{2}\sigma_{ij}\varepsilon_{ij} \approx \frac{1}{2}E_1\varepsilon_{y1}^2 \qquad (11)$$

2) After bone remodeling, it is assumed that axial strain(ε_{y2}) will approximate 2500 microstrain Young's modulus(E_2) at each location of the cancellous bone is still unknown, but the strain energy per volume has been estimated by Equation 11 and the 'approximate' final strain of ε_{y2} is known

$$U_{remodel} = \frac{1}{2}\sigma_{ij}\varepsilon_{ij} \approx \frac{1}{2}E_2\varepsilon_{y2}^2 \qquad (12)$$

The apparent density associated with this modulus(E_2) can be obtained from

$$E_2 = 2875\rho^3 \text{MPa for Young's modulus} \qquad (13)$$

Equation 13 has assumed a strain rate of 0.001 m/sec (Carter and Hayes 1977). Since the strain energy of an elastic structure under the same loading/boundary conditions is constant regardless of Young"s modulus(i.e. $U_{initial} = U_{remodel}$), the density obtained at Equation 13 per each element of the cancellous bone is

$$\rho^0 = 0.07\left(\frac{\varepsilon_{y1}}{\varepsilon_{y2}}\right)^{2/3} \qquad (14)$$

This equation is used to compute an initial density(ρ^0) distribution of the bone remodeling algorithm of Equation 9

3) With estimates for the apparent density distribution now obtained throughout the cancellous bone, Young's modulus(Equation 13) and strength of the cancellous bone (Equation 15) for each element are estimated at every iteration

$$\sigma_1 = 52\rho^2 \text{MPa for bone strength(Carter and Hayes 1977)} \qquad (15)$$

Through this technique, final density distribution is then obtained by the bone remodeling algorithm of Equation 9. As well, loads that cause local damage to cancellous bone can be identified.

RESULTS

The bone remodeling theory based on the volumetric strain was applied on two human femur models(Fig. 1-3) and a human normal spine model(Fig 4-7) with the frequency ratio($\frac{f}{f_{ref}}$) of 1.0 in Equation 9. Fig. 1 shows remodeling of the cancellous bone in a curved human femur. The right plot of Fig. 1 shows a volumetric strain distribution on the curved femur under a vertical compression of 2311 N, predicting that cancellous bone will resorb in the regions with low volumetric strain. This volumetric strain distribution is very similar to the bone density observed by Wolff (1892). Plot (1) of Fig. 3a predicts a volumetric strain distribution for the proximal model after an initial iteration. Further iterations of this model brought all strains within the physiologic range of 200-2500 microstrain(Plot(2) and Plot(3) of Fig. 3a). The convergence criterion with C_1 of 1.0E-3 (Equation 10) and Cm of 40 (Equation 9) was satisfied after 41 iterations (Plot (2) of Fig. 3a). When, alternatively, C_1 of 1.0E-4 and C_m of 40 were chosen, the apparent density distribution converged after 91 iterations (Plot (4) of Fig. 3a). The results after 41 iterations were nearly the same as the results after 91 iterations, showing good convergence with a smaller value of C_1. According to Equations 13 and 15, Young's modulus and strength of cancellous bone were obtained based on the computed bone apparent density (Plot (5) and (6) of Fig. 3a). Fig. 3b shows the convergence process with iterations for the proximal femur model. Error1 is the result from the left hand side of Equation 10. Error1 at any point in time is a measure of accuracy in the density distribution of the current model.

In the normal spine model(Fig. 4) under the convergence criterion with C_1 of 1.0E-4 and C_m of 40, only 3-4 iterations were required because the initial apparent density distribution was very closed to the final converged value according to Equations 9-15. Compressive behavior of the normal spine model was compared with the literature(Nachemson 1960, Brown *et al.* 1957, Berkson *et al* 1979, Kim and Goel 1988, Shirazi Adl *et al.* 1986, Tencer *et al.* 1982) (Fig. 5a, 5b). The curves of load-displacement and load pressure are close to the literature(Berkson *et al.* 1979). Under axial compression of 400 N, bone remodeling of the vertebral cancellous bone was explored(Fig. 6). Plot (1) of Figure 6 represents axial strain distribution of the L4 body after initial loading of 400 N. Volumetric strain was computed by summation of absolute values of normal strains(Plot (2) of Fig 6). After remodeling, the density distribution of the L4 body was extracted from the whole model(L3-L5) in order to avoid detrimental effects of the boundary conditions to the results. Apparent densities ranging from 0.122-0.435g/cm^3 were predicted by the bone remodeling theory(Fig 6). The apparent density distribution in Figure 6 shows that the peripheral border of the core is less dense, and the posterocentral region of the core is more dense in agreement with anatomical descriptions in Keller et al 1989. Plot(4) of Figure 6 shows that hydraulic pressure of both nuclei is about 0.26 MPa. The upper one is the nucleus between L3 and L4. The lower one is the nucleus between L4 and L5. Figure 7 predicts that the apparent density distribution of cancellous bone

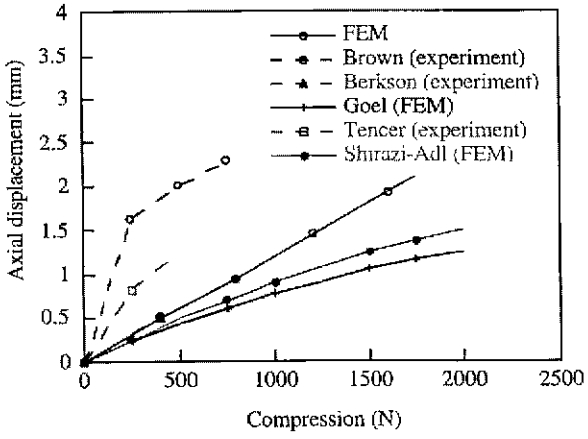

Fig. 5a Comparison of the normal spine model with several experiments in the experiments in the literature under axial compression. The load-displacement curve was in close agreement with Berkson *et al* (1979).

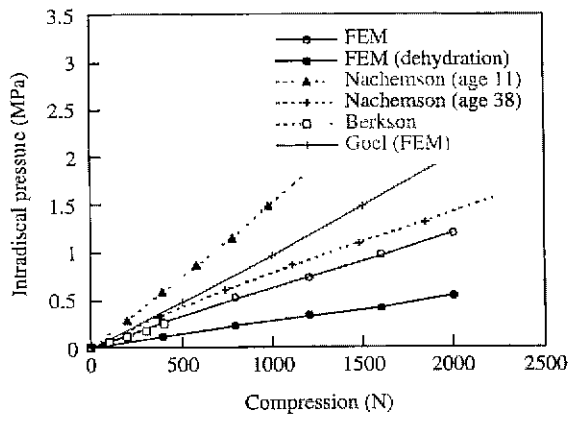

Fig. 5b. Comparison of the normal spine model with several experiments in the literature under axial compression. The load-pressure curve was in close agreement with Berkson *et al* (1979)

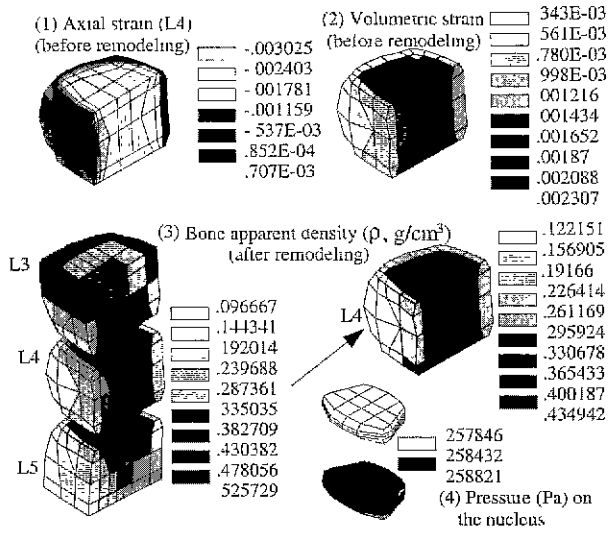

Fig. 6 Prediction of the apparent density for the vertebral cancellous bone under compression of 400 N

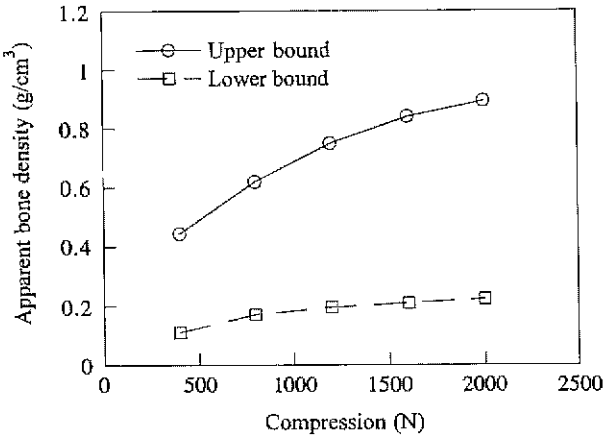

Fig. 7 The apparent density range of the vertebral cancellous bone for compressive loads. This result shows that the predicted range of apparent density for cancellous bone is 0.1-0.9(g/cm³)

varies with loading conditions within the range of 0.1-0.9 g/cm³. The upper bound of the density increases with the increase of the compression, showing wider range of the density distribution. This result shows that a person who is overweight or very active physically would have higher and wider density bone

The strain energy technique(Equations 11-14) can reduce computational time for bone remodeling studies with the spine model. The technique was used for determining an initial density distribution from which the final density distribution was obtained with only 3-4 iterations. Even for locations beyond the target range of 200-2500 microstrain, 3-7 iterations were enough for convergence of the spine model. In the proximal femur model, the boundary conditions and geometry are more complex so that axial compressive strain is not always dominant in the cancellous bone. Therefore, the strain energy technique was not as useful for the proximal femur model. Up to 91 iterations of the femur model were required before the convergence (Fig. 3b). If simple compression (axial strain) and bending (axial strain) were the only important factors then this technique would have been worked better

Discussion

The goal of this study was to formulate a method for predicting cancellous bone apparent density that did not include shear strains/stresses in its criterion. Shear strains /stresses can cause an increase in bone density with strain energy density theories and with effective stress/strain theories. Increases of this type are not consistent with most experimental observations. With the volumetric strain theory developed herein, shear strains/stresses were not considered. Carter *et al.*(1989) showed in a remodeling algorithm using the effective stress that the predicted apparent density distribution is similar to the experimental results(Wolff 1892), adjusting an exponential coefficient, M of the algorithm. Goel *et al.*(1995) showed in a spine model that Young"s modulus distribution is consistent with the experimental result(Keller *et al* 1989), using strain energy density. This consistency would be explained by the dominant axial strain of strain energy density even though shear strains are included. Turner *et al.*(1997) used a uniform strain criterion based on two principal strains in order to establish an algorithm for cancellous bone remodeling, which was similar to that suggested by Cowin(1984) and Cowin and Hegedus(1976). In the uniform strain criterion, principal strains were determined from all strain components including shear strain. Turner *et al* (1997) showed consistency of the result with experimental data, using two absolute principal strains. Carter(1987) insisted that most strain energy stored in bone reflects shear energy and that hydrostatic strain energy is just a little unless significant fluid flows, assuming negligible deformation of cartilage under even high hydrostatic pressure. Thus, he concluded that shear stresses rather than hydrostatic stresses are beneficial for bone gain in a bone remodeling algorithm, for which two stress invariants, the octahedral shear stress and the hydrostatic(dilatational) stress are used. He investigated a proximal femur using the finite element method in order to estimate trabecular

orientations(Fig. 7 of Carter (1987)) The left plot of Fig. 7 of Carter(1987), a bone normal stress distribution which is summation of compressive stress and tensile stress is very similar to the present result(Plot (4) of Fig 3a). In the present study without shear strains, the results(Fig 1,3,6) show consistency with experimental results in both spine and femur(Wolff 1892, Keller *et al.* 1989). The finite element models are linear isotropic heterogeneous This computation represents macroscopic analysis like material mechanics. Thus, the present models could not show microscopic analysis such as fluid shear on local bone surface and local marrow pressure. Though any shear strain is not included in this algorithm, a detrimental effect resulting from shear strains would exist In addition, the mesh structure of the present models was formulated in order to reduce computational time and memory space because more material properties of cancellous bone were needed as its mesh is denser. Denser mesh of the models would lead to more exact results. Despite of these limitations, the results obtained from the models were in qualitative agreement with observed values of cancellous bone density.

Tensile strain was assumed to have the same effect as compressive strain because differences between tensile strain and compressive strain on bone remodeling are not well known Since the results from this assumption are similar to the experimental results(Wolff 1892, Keller *et al.* 1989), the normal strains might relate with marrow pressure. According to Burger *et al* (1993), marrow pressure and marrow pressure gradient may influence osteoprogenitor cells in bone adaptation. Provided that the marrow pressure distribution caused by an external load is compared with strain distributions, the differences between tensile and compressive strains would be explored If the differences become known, the strain coefficients of Equation 5, c_x, c_y and c_z are adjustable. Nevertheless, this remodeling theory based on volumetric strain will be used for further investigation of bone remodeling and for design of implants.

If there is no external load, strain is zero and strain energy is zero. The strain energy technique of Equation 14, then, predicts zero initial density. The algorithm of Equation 9 predicts a final apparent density of zero, which is unrealistic. According to Jaworski and Uhthoff (1986), without load, bone density loss keeps 60-70% not complete bone loss Turner *et al.*(1997) suggested that this phenomenon would be explained by biological factors such as hormones and cytokines. However, these factors may cause marrow pressure to be maintained at a low level. That is, internal strain energy and normal strains would exist due to marrow pressure. Therefore, the bone loss of 60-70% might be explained by marrow pressure

The initial density is determined from the initial uniform axial strain induced by loads based on the strain energy of each element of cancellous bone The initial density is not uniform and varies with the location. The requirement for this algorithm is that all the volumetric strain be in the range of 200-2500 microstrain. If the initial strain is chosen at a lower level than the range, high levels of initial apparent density are obtained by Equation 14. Likewise, if the initial strain is chosen at a higher level than the range, the obtained initial density levels are lower than the initial density levels resulted from the low initial strain. The final density levels resulting from the high initial density is a little higher than that with low initial density It is important to note that the dead zone which is a range of strain stimuli that induce no net bone remodeling is considered. Consequently, with the dead zone of 200-2500 microstrain, this algorithm produces a solution that was non-unique to the initial density distribution of the model. That is, this algorithm is history dependent within the dead zone. The existence of a substantial range of strain stimuli at remodeling equilibrium hinders load determination. Non-uniqueness of this algorithm is consistent with the study (Weinans *et al.* 1989) Carter *et al.*(1989) shows that the density distribution is uniquely determined regardless of loading history. However, in the same conditions, some unique solutions have been developed(Goel *et al* 1995, Fischer *et al.* 1997). Uniqueness depends on the mathematical theory and the implementation of the algorithm.

In conclusion, a new remodeling theory for cancellous bone was formulated based on a volumetric strain criterion. This theory was verified on computer models of human spine and human femurs. The predicted density distributions were qualitatively in good agreement with the literature(Wolf 1892, Keller *et al.* 1989, Carter *et al.* 1977), showing that shear strains within bone are unlikely to govern the ossification The strain energy technique developed, in the present study, was very useful for saving computational time in convergence of the spine model. Therefore, these computational algorithms of the present study appear to be a useful approach to predict the apparent density distributions of cancellous bone.

Acknowledgments

The authors gratefully acknowledge assistance of Mary Checovich for understanding of bone structure

References

1. E.K. Antonsson and R.W Mann, "*Frequency Content of Gait*", J. of Biomechanics, Vol 18, pp.39-47, 1985
2. M H. Berkson, A Nachemson and A.B. Schultz, "*Mechanical Properties of Human Lumbar Spine Motion Segments-Part II: Responses in Compression and Shear; Influence of Gross Morphology*", J. of Biomechanical Engineering, ASME, Vol.101, pp.53-57, 1979
3. T. Brown, R.J Hansen and A.J. Yora', "*Some Mechanical Tests on the Lumbosacral Spine with Particular Reference to the Intervertebral Discs*", J. of Bone & Joint Surgery [Am], Vol.39, pp.1135-1164, 1957
4 E.H. Burger and J.P Veldhuijzen, Influence of mechanical factors on bone formation, resorption and growth in vitro. In Bone Bone Growth(edited by Hall, B.K.), CRC Press, Boca Raton, FL, pp.37-56, 1993
5. A. Cappozzo, T. Leo and A. Pedotti, "*A General Computing Method for the Analysis of Human Locomotion*", J of Biomechanics, Vol.8, pp.307-320, 1975
6. D.R. Carter, T E Orr and D.P. Fyhrie, "*Relationships between Loading History and Femoral Cancellous Bone Architecture*", J of Biomechanics, Vol 22, pp.231 -244, 1989
7. D.R Carter, "*Mechanical Loading History and Skeletal Biology*", J of Biomechanics, Vol.20, pp 1095-1109, 1987
8 D R. Carter and W C. Hayes, "*The Compressive Behavior of Bone as a Two-Phase Porous Structure*", J. of Bone & Joint Surgery, Vol.59A. pp.954-962, 1977
9. A.E. Churches and C.R. Howlett, The Response of Mature Cortical Bone to Controlled Time varying Loading. in Cowin S,C, Mechanical Properties of Bone (2ed), pp.81-92, 1981
10. D.D. Cody, E.B. Brown and M.J. Flynn, "*Regional Bone Density Distribution in Female Spines(T6 through L4)*", 38th Annual Meeting, Orthopaedic Research Society, pp.17-20, 1992
11. S.C. Cowin, Bone Mechanics(2ed), CRC Press, Inc. Boca Raton, Florida, 44-45, 1991
12. S C. Cowin, "*Mechanical Modeling of the Stress Adaptation process in Bone*", Calcified Tissue International, Vol 36, pp.S98-S103, 1984
13. S.C. Cowin and D H. Hegedus, Bone Remodeling I: Theory of the Adaptive Elasticity, J. of Elasticity, Vol.6, pp.313-326. 1976
14. J.M. Cox and R.F. Stevens, Low Back Pain, Mechanism, Diagnosis and Treatment. Wilhams and Wilkins, 4th ed, Fig. 2 25 2 38, 1985
15. K J. Fischer, C.R. Jacobs. M.E Levenston and D.R, "*Observation of Convergence and Uniqueness of Node-Based Bone Remodeling Simulations*", Annals of Biomedical Engineering, Vol 25. pp.261-268, 1997
16. H.M. Frost, Bone Mass and the Mechanostat: A Proposal, Anatomical Record, 219, 1-9, 1987
17 D.P. Fyhrie and M B. Schaffler, "*Failure mechanisms in Human Vertebral Cancellous Bone*", Bone, 15, 105-109, 1994
18. V K. Goel, S.A. Ramires, W. Kong and L.G. Gilbertson. "*Cancellous Bone Young's Modulus Variation within the Vertebral Body of a Ligamentous Lumbar Spine-Application of Bone adaptive Remodeling Concepts*", ASME J. of Biomechanical Engineering, Vol. 117, pp.266-271, 1995
19. J.O. Grante JO, "*Tensile properties of the Human Lumbar Annulus Fibrosis*", Acta Orthopaedica Scandinavica Supplement 100, 1967
20. L.J. Grobler, P.A. Robertson, J.E. Novotny and M.H. Pope, "*Etiology of Spondylolisthesis: Assessment of the Role Played by Lumbar Facet Joint Morphology*", Spine, Vol.18. pp.80-91, 1993
21. O. Grundenes and O. Reikeras, "*Effects of Instability on Bone Healing. Femoral Osteotomies Studied in Rats*", Acta Orthopaedica Scandinavica, Vol.64, pp.55 -58, 1993
22. Z.F. Jaworski and H.K. Uhthoff, "*Reversibility of Nontraumatic Disuse Osteoporosis during its Active Phase*", Bone, Vol 7, pp.431-439, 1986
23. T.S. Keller, T.H. Hansson, A.C. Abram, D,N Spengler and M.M Panjabi, "*Regional Variations in the Compressive Properties of Lumbar Vertebral Trabeculae. Effects of Disc Degeneration*", Spine, Vol 14, pp.1012-1019, 1989
24 Y.E. Kim and V.K. Goel, "Biomechanics of Chemonucleolysis", The winter annual meeting of the ASME, Vol 9, pp.461-471, 1988
25. L.E. Lanyon and C.T. Rubin, "*Static versus Dynamic Loads as an influence on Bone Remodeling*", J. of

Biomechanics, Vol.17, pp.897-900, 1985
26. F Marchand and A.M. Ahmed, "*Investigation of the Lamunate Structure of Lumbar Disc Annulus Fibrosis*", Spine, Vol.15, pp.402-410, 1990
27. A. Nachemson A, "*Lumbar Intradiscal Pressure*", Acta Orthopaedica Scandinavica, Supplement 43, pp.1-140, 1960
28. M.M. Panjabi, V.K. Goel, K Takata, J. Duranceau, M. Krag and M Price, "*Human Lumbar Vertebrae-Quantitative Three-Dimensional Anatomy*", Spine, Vol.17, pp.299-306, 1992
29. M.M. Panjabi, T Oxland, K. Takada, V.K Goel, J. Duranceau and M. Krag, "*Articular Facets of the Human Spine: Quantitative Three-Dimensional Anatomy*", Spine, Vol.18, pp.1298-1310, 1993
30. J.C. Rice, S.C. Cowin and J A. Bowman, "*On the Dependence of the Elasticity and Strength of Cancellous Bone on Apparent Density*", J of Biomechanics, Vol.21, pp.155-168, 1988
31. A Shirazi-Adl, C. Suresh, A.M. Ahmed and S.C Shrivastava, "*A Finite Element Study of A lumbar Motion Segment Subjected to Pure Sagittal Plane Moments*", J. of Biomechanics, Vol 19, pp.331-350, 1986
32. D L. Skaggs, M. Weidenbaum, J.C. Latridis, A. Ratcliffe and V.C. Mow, "*Regional Variation in Tensile Properties and Biochemical Composition of the Human Lumbar Annulus Fibrosis*", Spine, Vol.19, pp.1310-1319, 1994
33. A.F. Tencer, A M Ahmed and D.L. Burke, "*Some Static Mechanical Properties of the Lumbar Intervertebral Joint, Intact and Injured*", J. of Biomechanics, Vol.104, pp 193-201, 1982
34. C.H. Turner, A. Anner and R M V Pidaparti, "*A Uniform Strain Criterion for Trabecular Bone Adaptation: Do Continuum-Level Strain Gradients Drive Adaptation?*", J. of Biomechanics, Vol.30, pp 555-563, 1997
35. H Weinans, R. Huiskes and H.J. Grootenboer, "*Effects of Fit and Bonding Characteristics of Femoral Stems on Adaptive Bone Remodeling*", ASME J. of Biomechanical Engineering, Vol.116, pp.393-400, 1994
36. A A White and M.M. Panjabi, "*Clinical Biomechanics of the Spine*", 2nd edition, JB Lippincott, Philadelphia, 1990
37. J. Wolff, The law of Bone Remodeling, Translated by Paul Maquer (1986), Springer Verlag Berlin Heidelberg, 1892